World Conference on Timber Engineering Oslo 2023

ON THE UTILISATION OF THE WORKSPACE OF AN INDUSTRIAL ROBOT FOR MILLING STRUCTURAL TIMBER COMPONENTS – EXPERIMENTAL TRIALS WITH DIFFERENT ARM POSITIONS AND EVALUATION OF MACHINING QUALITY

Marc Pantscharowitsch[1], Finn Linzer[2], Hans-Berndt Neuner[3] Benjamin Kromoser[4]

ABSTRACT:

Within subtractive manufacturing of timber construction components, industrial robots equipped with a milling spindle hold great potential for efficiency increases and new production methods. A key difference to modern joinery machines is the larger workspace, especially in the horizontal and vertical direction. This pushes the limits for the dimensions of workpiece cross sections and allows for newly thought-out workpiece placement and possibilities for batch processing. However, a basis must be created to assess the quality and to evaluate the effects of different robot positions on the machining quality. The subject of this paper is therefore the machining of pockets in glued laminated timber using the same parameters yet in two test series: A) four different robot positions and tool orientations B) the reach is set to four different values with each two workpiece orientations. The processing quality is then assessed based on four different scales of magnitude: 1) nominal/actual geometry comparison; 2) optical and haptic surface quality assessment; 3) stylus method surface roughness measurements; 4) 3D scans. The results show effects of the position especially in machining directions influenced by longer static levers and mass inertia. Nevertheless, compared to reference workpieces the machining quality is competitive.

KEYWORDS: 3D Scan, Automation in Construction, Glued Laminated Timber, Glulam, Quality Assessment, Robotic Manufacturing

1 INTRODUCTION

Industrial robots (IR) are already state of the art in the automotive and electronics industries [1]. Equipped with a machining spindle they have a high potential to increase the efficiency of subtractive manufacturing of engineered timber construction components. The advantages of IRs over the widely used joinery machines (JM) lie in the lower acquisition costs, the higher technological development and innovation, as well as the availability of robots and spare parts. In terms of their machining properties, they offer opportunities to increase productivity through higher degrees of freedom (DOF), larger workspace and higher flexibility. [2] To determine the applicability of IRs in engineered timber construction, a comprehensive scientific study is required. Therefore, as a first step, the quality of the machining results of IRs was analysed by the authors [3]. The milling of elementary geometries such as lines, rings and pockets using an IR was investigated and showed that the surface quality is satisfactory for the use in timber construction. Furthermore, the geometry and surface quality of milled pockets was compared to pockets manufactured with JMs. The comparison showed that the mean machining quality of the IRs is 11.52 % higher (indicated by the quality deviation value QDV) than that of the JMs. [4] Following these results, the same assessment methods were applied to another type of timber connection: the tenon. This study showed a 24.53 % higher machining quality of the JM compared to the highest quality IR specimen. Nevertheless the surface quality and geometry precision of the IR manufactured specimens was still high enough to meet industry standards. [5]

Having demonstrated the feasibility of subtractive machining using IRs by studying elementary geometries and application examples (pockets and tenons), this investigation looks into the potential of the larger workspace available when using IRs, specifically if the machining quality meets the requirements in terms of dimensional accuracy and surface quality. The idea is to identify potential causes for instability and ultimately lower machining quality.

2 EXPERIMENTAL SETUP

The machines, tools, the specific machining parameters, and the investigated specimens within the two test series are described in this section. In order to investigate the potential of IRs a reference with state of practice

[1] Marc Pantscharowitsch, University of Natural Resources and Life Sciences, Vienna (BOKU), Austria, marc.pantscharowitsch@students.boku.ac.at
[2] Finn Linzer, Technical University Vienna (TUW), Austria, finn.linzer@tuwien.ac.at
[3] Hans-Berndt Neuner, Technical University Vienna (TUW), Austria, hans.neuner@tuwien.ac.at
[4] Benjamin Kromoser, University of Natural Resources and Life Sciences, Vienna (BOKU), Austria, benjamin.kromoser@boku.ac.at

https://doi.org/10.52202/069179-0082

machinery, in this case JMs, needs to be additionally looked into.

2.1 MACHINES AND TOOLS

First the machines and tools of both used within the investigations are described.

2.1.1 IR

The BOKU robot laboratory (Figure 1) is the home of an ABB IRB 7600-325 IR mounted on an ABB IRBT 6004 external linear axis with the following properties: reach 3.10 m; payload 325 kg; position repeat accuracy 0.19 mm, trajectory repeat accuracy 0.4 mm (according to manufacturer) [6]. The IR can be equipped with various end effectors (EE), however within this study a HSD ES951 A 1112 S spindle with 13.2 kW and 10.5 Nm at 12,000 rpm was used. The machining was done with an insert cutter by Leitz (tool ID: 41927) as depicted in Figure 2 with a diameter Ø of 40 mm, an edge height of 160 mm, and two Z2 carbide milling inserts (HeliCut 11 mm x 11 mm x 1,5 mm and one drill cutting edge), with a cutting angle of 20°, a clearance angle of 20° and helix angle of 15° complemented by the HSK F-63 tool holder. The cutting inserts were unused before and showed no tool wear. A solid 2,400 mm by 1,200 mm steel worktable was used as the machining bed, comprising of 24 lamellae parallel to the short side with slots in between to allow for workpiece attachment.

Figure 1: *BOKU robot laboratory with ABB IRB 7600-325 industrial robot mounted on ABB IRBT 6004 external linear axis with the end effector (EE): HSD ES951 A 1112 S and the steel worktable in the back.*

2.1.2 JM

The reference workpieces were machined on a Hundegger k2i joinery machine (JM) using a 5-axis universal milling unit (15 kW up to 5,200 rpm) at the facilities of Rubner Holzbau GmbH. The tool used was an end mill with a diameter Ø of 36 mm, and a length L of 150 mm.

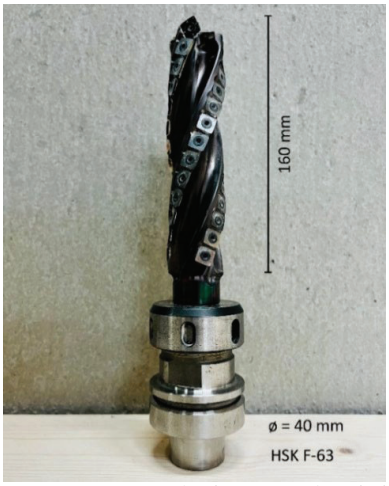

Figure 2: *Leitz insert cutter (tool ID: 41927) with diameter = 40 mm, edge height = 160 mm, 2 x Z2 carbide milling inserts (HeliCut 11 x 11 x 1,5 mm and 1 x drill cutting edge), cutting angle = 20°, clearance angle = 20°, helix angle = 15° and HSK F-63 tool holder.*

2.2 MACHINING PARAMETERS

As not only the used machinery but also the specific machining parameters are of importance within the potential assessment, a statement in regard to the latter is given below.

2.2.1 IR

The machining parameters of the IR were set the same for both test series. The spindle speed was set to 17,900 rpm, with a feed rate of 5,500 mm/min, a radial depth of cut of 35 mm and an axial depth of cut of 20 mm while climb cutting. The machining strategy is visualised blue in Figure 3.

2.2.2 JM

The authors did not have any influence on the machining parameters of the JM as they were set according to the machine operator's experience, relying on best practice and recommendations of the tool manufacturer: spindle speed = 4,000 rpm, feed rate = trajectory speed 5, unknown radial depth of cut, axial depth of cut = 20 mm while climb and conventional cutting. The trajectory speed, as reported by the machine manufacturer Hundegger in an interview [7], is indicated by an integer value from 1 to n. This integer represents the ratio of the set machining speed to the maximum machining speed, which is unique for each toolpath. When looking at a given machining process including cutting, milling and conveying processes and increasing the trajectory speed, the cutting and milling time is reduced but not the conveying time. Therefore, it is not possible to express the speed in SI units as there is no linear relationship. The machining strategy and trajectory of the tool centre point (TCP) are marked red in Figure 3.

2.3 SPECIMENS

The investigated workpieces consisted of four pockets (263 mm x 111 mm x 20 mm) with rounded corners (radius R = 20 mm) as presented in Figure 3. The

https://doi.org/10.52202/069179-0082

machining tests of both series were carried out on glued laminated timber (GLT: Gl24h, spruce, Picea abies L. Kars.).

2.3.1 Reference series

As a reference, two specimens were machined by the previously described JM on a GLT beam workpiece (cross section 200 mm x 200 mm).

2.3.2 Series A

Series A was conducted on a GLT beam with the cross-sectional dimensions of 200 x 200 mm, with the direction of the fibres and lamellae parallel to the long edge of the beam and pockets. The pockets were machined once at the end of the beam on four different opposing surfaces, each with a different orientation. The machining parameters were kept unchanged throughout the investigations, allowing for a comparison of the milling results depending on the robot position as shown in Figure 4. The workpiece was placed upon two vertical supports during all machining trials to achieve the reachability of the workpiece when machining overhead (Figure 4 D).

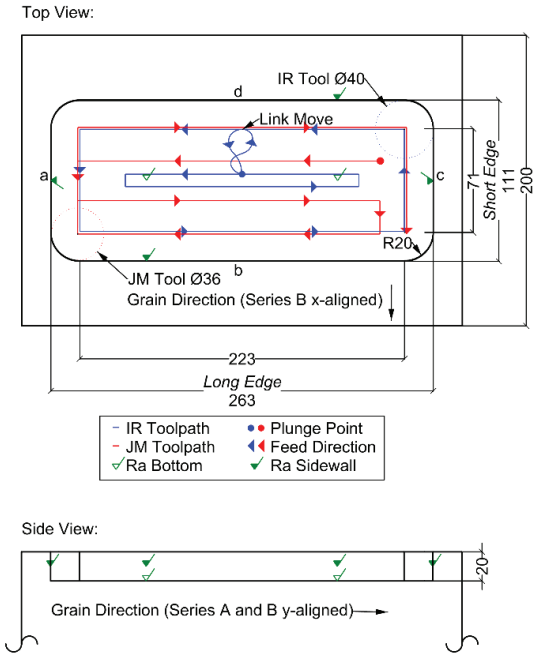

Figure 3: *Specimen [mm]: machined pocket with radial corners. The trajectory of the tool centre point of the toolpath, plunge point and feed direction is represented in blue (IR) and red (JM). Average surface roughness measurement points are marked green. Workpiece of series A and reference series: GLT beam (cross section 200 mm x 200 mm).*

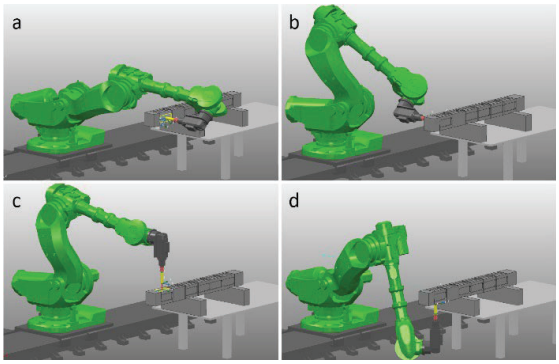

Figure 4: *ABB IRB 7600-325 industrial robot in the four different analysed positions and orientations. A) Long reach, B) Short reach, C) Vertical, D) Overhead.*

2.3.3 Series B

The trials of Series B were conducted on GLT workpieces measuring 2,000 mm x 600 mm x100 mm with the fibre direction parallel to the long edge of the workpiece. This series was subdivided into two subseries. In the first subseries, the pockets were aligned parallel to the long edge of the workpiece (further referred to as y-aligned due to the robots` coordinate system visualised in Figure 5). In the second subseries, the pockets were aligned normal to the long edge of the workpiece (further referred to as x-aligned). Each alignment and reach were machined three times for redundance. The reason for the two different investigated orientations of the specimens relative to the grain is not due to the anatomical structure of the wood but rather the robot motion direction while machining. With the pockets being y-aligned, the longer longitudinal motion requires the robot to increase its reach, while for the x-aligned pockets it is demanding the robot primarily to move laterally and also needs to turn. In Figure 5 top, the workpiece placement in the robot workspace is illustrated with the IR located directly over the central axis of the pockets in y-direction. The four investigated workpiece placement positions are visualised in Figure 5 and were chosen to exploit the entirety of the workspace limits. Position 1 was chosen as close as possible to the robot base while position 4 represented the opposite (farthest away placement still allowing for a undisturbed milling). Positions 2 and 3 were evenly distributed between 1 and 4. As a result, the reach of all four positions varies between the x- and y-aligned test series, as listed in Table 1. Reach is defined by the distance between the robot base (centre of rotation of axis 1 as marked with 0 mm reach in Figure 5 top) and the mid of the pocket. To allow for the investigations of the defined placements with an adequate secure stability, the worktable was extended (marked red) by moving every second lamellae in y- direction.

https://doi.org/10.52202/069179-0082

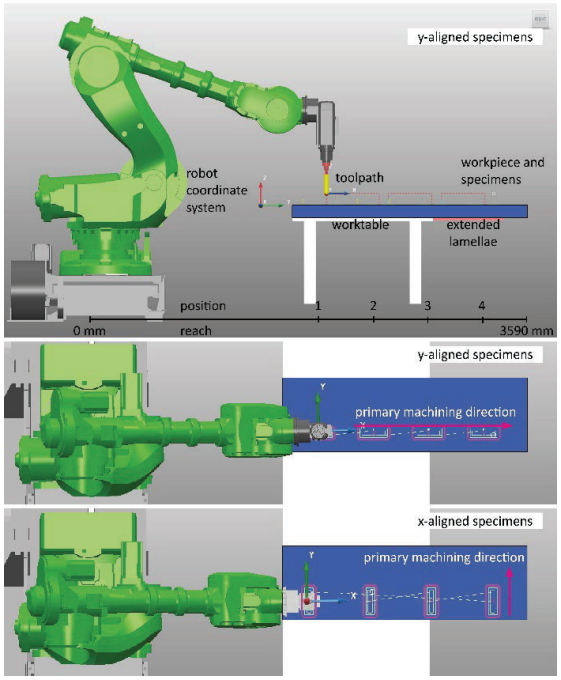

Figure 5: *Top: Workpiece placement, robot positions and reach of y-aligned specimens. Mid: Top view of workpiece placement and primary machining direction of y-aligned specimens. Bottom: Top view of workpiece placement and primary machining direction of x-aligned specimens.*

Table 1: *Specimens positions. * reach is measured from robot base (centre of rotation of axis 1 as marked with 0 mm reach in Figure 5 top) to specimen centre parallel to the y-axis of the robot coordinate system. Δ describes the distance between the positions in y-direction.*

Position	Specimen x-aligned	Reach x-aligned* [mm]	Specimen y-aligned	Reach y-aligned* [mm]
Δ	-	*500*	-	*450*
1	X1	1806	Y1	1882
2	X2	2306	Y2	2332
3	X3	2806	Y3	2782
4	X4	3306	Y4	3232

3 EVALUATION METHODS

In Austria, manufacturing requirements for structural timber can be found in ÖNORM EN 336 [8], with the dimensional accuracy specified in Table NA.L.5 in Eurocode 5 DIN EN 1995 [9] while characteristics for timbre materials like GLT are defined in ÖNORM EN 14080 [10]. Despite these regulations, surface roughness and local geometrical deviations are not considered within the regulations. To evaluate the influence of the different positions and reaches of IRs, the following references and criteria were considered.

3.1 DIMENSIONAL ASSESSMENT

Dimensional measurements were carried out on all specimens of Series A and B using two methods: by hand and by laser profile scans. The results of both methods were combined into mean values before calculating the actual-nominal deviation. Subsequently, the utilisation factor (UF) of each dimension (Length L, Width W, Height H) of every specimen was calculated based on the actual-nominal deviation and regulations specified by ÖNORM EN 14080 [10] (height h ≤ 400 mm: +4 to -2 mm and length l ≤ 2 m: ±2 mm). Note, these regulations do not specify timber in connections. Finally, the cumulated utilisation factor (CUF) of each individual specimen was calculated by determining the mean value of the three individual UFs.

3.1.1 Measurement by Hand

The dimensions (L, W, H) of all specimens were measured by hand using a carpenter´s square. Each measurement was taken three times to avoid discrepancies before the mean values were calculated.

3.1.2 Laser profile Scans

The profile scans were performed using a Keyence LJ-X8900 profile scanner. Mounted to the EE of the robot, the laser profile is aligned parallel to the y-axis of the robot coordinate system (as pictured in Figure 5) producing 2D data. Combined with the robot motion in x-direction, 16,000 profiles are combined into one 3D image. The accuracy in the x-direction is dependent on the robots` speed and the scanners` capture frequency, or in other words the distance travelled in acquiring all the profiles, resulting in this case in 4,000 mm / 16,000 profiles = 0,25 mm. In the y-direction along the profile, the accuracy is given with 25 µm and in the z-direction with 10 µm. The collected data was analysed by the Keyence controller firmware for LJ-X8000 (3D mode) version 1.4. The specimens lengths and widths were measured with the tool gap pitch (edge pairs) from light to dark with 55% edge sensitivity, edge filter width 50 and lower edge intensity 10. The specimen´s pocket depths were assessed with the tool height measurement where the peak-to-peak height was extracted.

3.2 QDV

Currently, there are neither normative regulations nor a consensus within science on an objective assessment system for machined surfaces in timber construction [11]. Therefore, the authors have introduced the quality deviation value (QDV) [3], which is composed of optical and haptic assessment of the geometry as well as the surface roughness R_a measured using the stylus method in addition to optical and haptic inspection.

3.2.1 Geometry Assessment: Optical and Haptic

The geometric quality was assessed both optically and haptically evaluating z-deviations in the bottom area and x- / y- deviations in the sidewall surfaces. The subjective optical and haptic inspection was conducted by two parties to increase objectivity. The characteristics were described by three values: “height criterium” for z-deviations in the bottom area, “lateral criterium short edge” and “lateral criterium long edge” for x- / y- deviations in the sidewall areas with QDV ratings from 1-6 (lower values indicating lower quality). The optic and haptic assessment also includes wood surface defects such as fuzzy grain, which describes wood fibres or fibre collectives that protrude from the surface, or torn

https://doi.org/10.52202/069179-0082

fibre, defined by torn-out wood pieces that do not break directly when cut [12].

3.2.2 Roughness Assessment: Optical and Haptic

Optical and haptic inspection was carried out additionally to analyse the surface roughness caused by the anatomical structure of the wood and machining of the three investigated areas (bottom and short/long sidewalls). Again, the inspection was conducted by two independent parties. As a reference, Figure 6 shows various machined surfaces with associated QDV ratings (min = 1 – good quality, max = 6 – poor quality).[3]

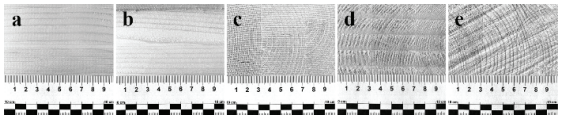

Figure 6: *Assessment of the optical/haptic surface roughness, dependent on the growth direction and machining process. Bottom surface and long edge sidewall surfaces (parallel to the grain): (a) radial/tangential planed, QDV = 1 (b) radial/tangential robot milling with 40 mm insert cutter, QDV = 2. Short edge sidewall surfaces (perpendicular to the grain): (c) axial blade saw cutting, QDV = 3 (d) axial manual chain saw cutting, QDV = 6. [3]*

3.2.3 Surface Roughness Measurement

The stylus method was used to measure the surface roughness of all inspected areas (bottom and short/long sidewalls). The measuring device was a MarSurf PS 10 (PHT 350, 2 µm probe) as shown in Figure 7 with the following settings: evaluation length Lt: 12.50 mm, Gaussian profile filter Ls: 8.00 µm, Lc = 2.5 µm, number of measured subsections N = 5 measuring velocity Vt: 0.5 mm/s, measured points: 30,000. The average surface roughness R_a was chosen as the measured quantity and the data acquisition was performed according to ÖNORM EN ISO 4287 [13] and ÖNORM ISO 16610 [9]. The measured values were scaled by applying a scaling factor (= maximum measured R_a value divided by 6) in order to not distort the QDV.

Figure 7: *MarSurf PS 10 device collecting surface roughness data on bottom area of a specimen of Series B. The stylus is located below the bottom left black tube.*

To increase the validity and reduce the influence of anisotropic and inhomogeneous wood properties, three measurements were conducted on each measuring point. The location of measurement points is depicted in Figure 3 and was marked on the specimens to increase the transparency of the study as recommended by Gurau and Irle [11].

3.3 3D SCANS: POINT CLOUDS

For the micro-scale assessment of the machining irregularities and tracing of tool paths, 3D point cloud scans of Series A were performed. First assessments can be found in [4], [5]. A Leica Absolute Tracker with a Leica T-Scan TS 50-A was used during the examinations to create a point cloud consisting of approximately 1 million points per specimen with the measurement uncertainty to plane surfaces of 80 µm (2 sigma). The data was analysed in the following three steps:
1) Division of the pocket geometry into five sections as presented in Figure 3: bottom surface, left short edge side wall a, lower long edge side wall b, right short edge side wall c and top long edge side wall d.
2) Analysis of the obtained point clouds using the CloudCompare software in the following steps: 2a) Fitting a reference plane to each machined surface a-d and bottom. 2b) Calculation of the difference of each point of the point cloud normal to the reference plane and subdivision into classes. 2c) Assessment of the number of points per class and visualisation in a histogram including a gaussian function graph.
3) Assessment of the data using RStudio. 3a) Preparation and inspection of the QQ-plots of the histograms for normal distribution as this is a precondition for the Wilcoxon rank-sum test. 3b) Assessment of the date using the Wilcoxon rank-sum test to compare the congruency of two identical sections of two different pockets (e.g. bottom surface specimen 1 with bottom surface specimen 2) by their mean values per class. As the null hypothesis states that the true location shift is equal to 0, its rejection ($p < 0.05$) indicates a major difference between the inspected surfaces. The Wilcoxon rank-sum test was performed on pairs of all five congruent areas of Series A specimens Vertical vs. Overhead and Series A specimens Short reach vs. Long reach.

4 RESULTS

In this section, the results of each series and evaluation method are reported.

4.1 SERIES A

Series A concludes the investigation of the four different robot positions Vertical, Overhead, Short reach and Long Reach.

4.1.1 Dimensional Assessment

The results of the dimensional assessment (measurements by hand and laser scanner) are displayed in Figure 8 as nominal-actual deviations. The mean deviations and UF, as described in Section 3.1, were L = 1.85 mm (UF = 92%), W = -1.47 mm (UF = 74%) and H = -0.33 mm (UF = 25%). The CUF per specimen was Vertical = 64%; Overhead = 60%; Short reach = 68% and Long reach = 62%. Calculated differences of CUF for the compared pairs resulted in 4% higher CUF when machined Vertical

https://doi.org/10.52202/069179-0082

against Overhead and 6% higher when machining Short reach against Long reach.

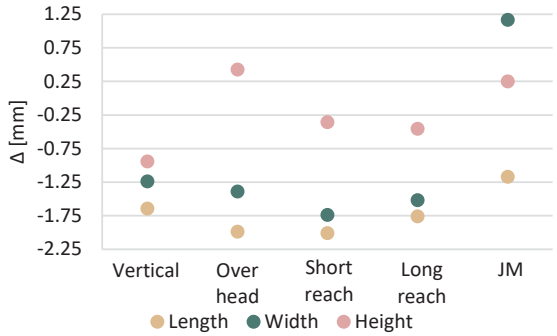

Figure 8: *Nominal-actual deviations for specimens of Series A.*

4.1.2 QDV

The results of the QDV assessment for Series A are displayed in Figure 9 with higher values indicating more deviations and irregularities. The calculated mean QDV of Series A is 19.68 (maximum achievable value 42), while the mean surface roughness R_a equalled 4.7 µm. The mean result of the JM machined reference specimens is also included. The main differences of QDV were observed for the height and lateral criteria and optical and haptic surface roughness assessment.

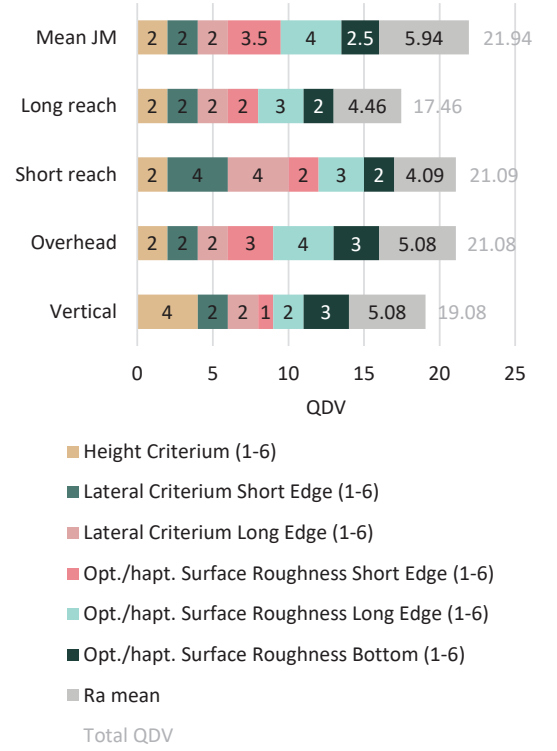

Figure 9: *Quality deviation value (QDV) of individual specimens of Series A. Higher QDVs represent more deviations and irregularities.*

4.1.3 3D Scans

The results of the Shapiro-Wilk normality test (see Table 2) for all inspected surfaces are $p < 0.05$ so the null hypothesis is denied and no normal distribution is present. This is a precondition for the following Wilcoxon rank-sum test for the statistical comparison of two surfaces.

Table 2: *Shapiro-Wilk normality test results. P-values < 0.05 indicate that the null hypothesis is denied and no normal distribution is present.*

Specimen	Inspection area	W	p
Vertical	bottom	0.94628	4.36E-05
Vertical	a	0.85753	6.96E-03
Vertical	b	0.9641	4.00E-07
Vertical	c	0.93584	1.08E-08
Vertical	d	0.95862	1.34E-02
Overhead	bottom	0.77529	2.20E-16
Overhead	a	0.92619	4.06E-03
Overhead	b	0.93049	8.06E-07
Overhead	c	0.90321	1.43E-12
Overhead	d	0.96777	4.07E-04
Short reach	bottom	0.88432	2.20E-16
Short reach	a	0.8998	7.76E-06
Short reach	b	0.88563	2.48E-09
Short reach	c	0.90724	4.40E-06
Short reach	d	0.9673	1.27E-04
Long reach	bottom	0.95337	2.20E-16
Long reach	a	0.92536	4.91E-08
Long reach	b	0.96997	1.80E-04
Long reach	c	0.93647	6.48E-06
Long reach	d	0.93212	9.72E-06

The Wilcoxon rank-sum test was conducted to compare two surfaces of the same type (e.g.: sidewall a). The results in Table 3 represent the significance level for every pair. If $p < 0.05$, the null hypothesis (no significant difference) is denied. In this comparison, the sidewall a of Vertical and Overhead machining and bottom areas of the Short reach and Long reach specimens are significantly different. All other pairs show no significant difference in the point to reference plane distance. As presented in Figure 10 the point cloud to reference plane distances overlaid with an image of the specimen clearly reveal the tool marks and micro-scale irregularities.

Table 3: *Wilcoxon rank-sum test results.*

Specimen and inspection area	W	p	Significant difference
Vertical vs. Overhead			
bottom	90022	0.8573	No
a	2914	0.03946	Yes
b	72058	0.6398	No
c	78927	0.8323	No
d	18428	0.5463	No
Short reach vs. Long reach			
bottom	379543	0.003089	Yes
a	25497	0.0783	No
b	27214	0.07479	No
c	23762	0.1591	No
d	20904	0.1349	No

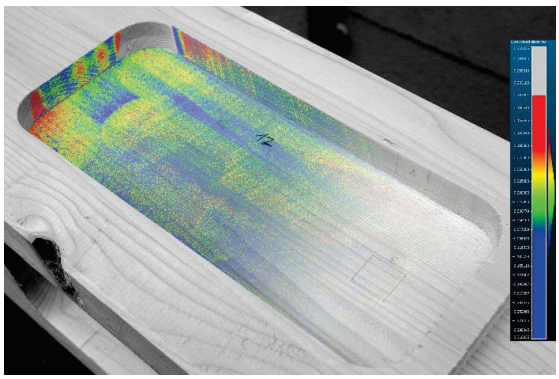

Figure 10: *Specimen 12 with overlaid point cloud with the scalar field indicating calculated point to reference plane distances.*

4.2 SERIES B

Series B includes the analysis of four different reach positions and two different workpiece alignments.

4.2.1 Dimensional Assessment

The results of the dimensional assessment are displayed in Figure 11 as nominal-actual deviations for each measurand and specimen orientation. The mean deviations and UF for the whole test series were L = 1.10 mm (UF = 55%), W = 0.66 mm (UF = 33%) and H = 0.55 mm (UF = 33%). Differentiated for x-aligned specimens the mean deviations and UF were L = 1.33 mm (UF = 66%), W = 0.57 mm (UF = 29%) and H = 0.34 mm (UF = 17%). The CUF per specimen was X1 = 39%; X2 = 32%; X3 = 32% and X4 = 47%. And for y-aligned specimens: L = 0.88 mm (UF = 44%), W = 0.76 mm (UF = 38%) and H = 0.99 mm (UF = 49%). The CUF per specimen was Y1 = 31%; Y2 = 45%; Y3 = 45% and Y4 = 54%. With increased reach, the overall CUF of both alignments and three dimensions increased from 35% to 50%.

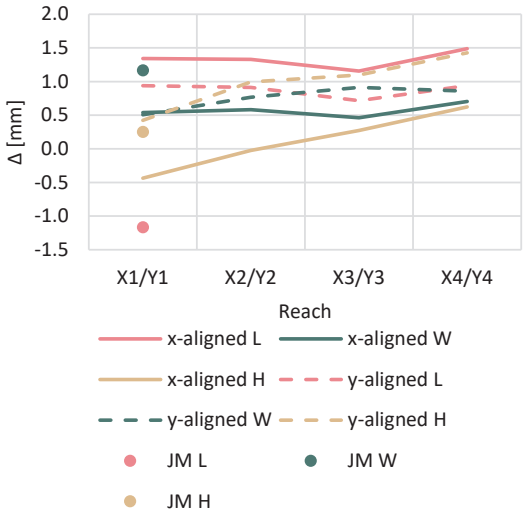

Figure 11: *Nominal-actual deviations and reach for x- and y-aligned specimens of series B as lines and JM reference values as points. Length deviations are marked red, width deviations green and height deviations brown.*

4.2.2 QDV

The QDV assessment was also conducted for Series B with the results displayed in Figure 12 with, as in Series A, the mean results of the two JM specimens also included. The mean QDV of Series B equals 19.52 (maximum value 42), with the x-aligned specimens showing a higher value with 20.55 and therefore more deviations, while the y-aligned show a value of 18.48 (10% difference). The total mean surface roughness is R_a = 4.1 µm, with again the x-aligned specimens showing higher values than the y-aligned specimens with 4.6 µm and 3.7 µm, respectively. The inspection of the short sidewall areas shows a sum over all four specimens and two values (lateral criterium and optical and haptic surface roughness) of QDV = 19 for x-aligned specimens and QDV = 20 for y-aligned indicating slightly higher deviations for y-aligned specimens.

In Figure 13 the QDV of Series B is plotted against the four positions with different reaches for both, the x- and y-aligned specimens. The trend line indicates rising QDV with increased reach implicating more deviations for both alignments. Further, the y-aligned specimens show lower QDV than the x-aligned. As a reference the mean QDV of the JM specimens is marked brown. All specimens of Series A and B except one (x-aligned reach 4) are below those of the JM.

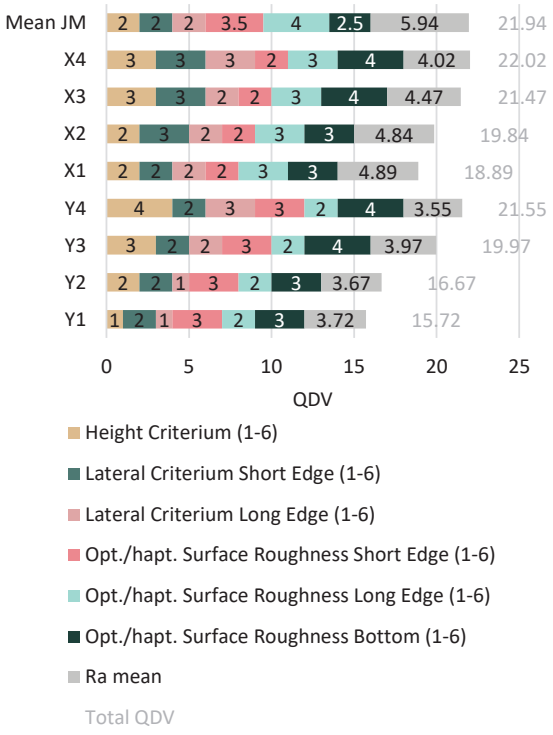

Figure 12: *Quality deviation value (QDV) of individual specimens of Series B. Higher QDVs represent more deviations and irregularities.*

When inspecting the results of the profile line scans, presented in Figure 14, the previously reported change in the pocket depth with varied reach becomes visible. It should however be noted that the height deviations listed

https://doi.org/10.52202/069179-0082

in Figure 11 were measured relative from the bottom to upper edge of the specimens while Figure 14 displays global height differences that could be affected by an uneven workpiece and worktable. The images in Figure 14 are primarily a valuable tool to trace tool marks and irregularities such as fuzzy grain defect that is visible in at least one spot of every specimen where tool trajectories overlap. The bottom pocket machined with a reach of 1806 mm (X1) shows two spots with fuzzy grain defects. Torn fibre defects occur within the specimens with maximum reach in the bottom right corner of the pocket.

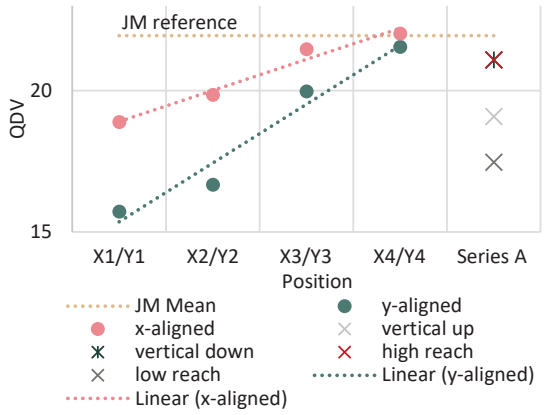

Figure 13: *Quality deviation value (QDV) of x- and y-aligned specimens of Series B. Additionally, Series A values are marked with crosses and the reference specimens machined by JM are marked as lines. Higher QDVs represent more deviations and irregularities.*

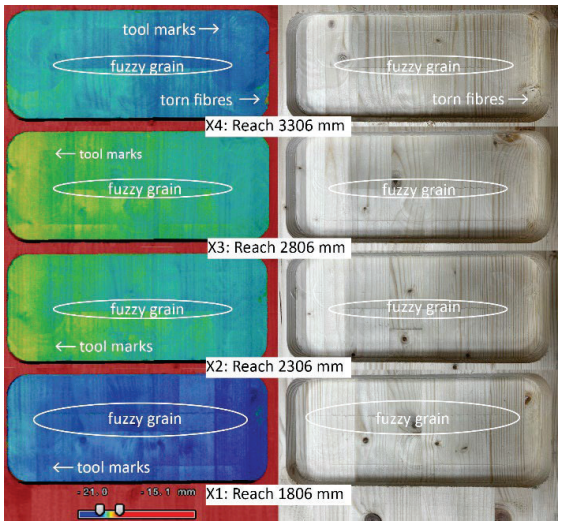

Figure 14: *Topography (left) and photographs (right) of series B x-aligned. The reach was increased from bottom to top. Note: The displayed height is global height difference between sensor and specimen.*

5 DISCUSSION

5.1 General

The dimensional deviations of all specimens of Series A apart from Short reach height and B are within the regulations´ margins defined in ÖNORM EN 14080 [10] with a maximum of -2 mm (UF = 100%).When comparing the dimensional deviations of the IR machined Series A (mean deviations L = 1.85 mm, W = -1.47 mm, H = -0.33) and B (mean deviations L = 1.10 mm, W = 0.67 mm and H = 0.55 mm). with the JM (mean deviations L = 1.17 mm, W = -1.17 mm and H = 0.25 mm) machined references, the results of the JM are more evenly distributed around zero deviation while having a similar span (span IR = 2.44 mm, span JM=2.33 mm). Overall, the achieved machining quality can be considered as sufficiently high with mean deviations of the JM = 0.86 mm as a reference and with slightly higher deviations with Δ = 0.19 mm the mean deviations of the IR = 1.05 mm. The QDV of all except one IR machined specimen is lower than for the JM machined indicating less irregularities. However, the IR tools were previously sharpened as the tool wear of the JM is not known. The main conclusion is therefore that the required machining accuracy and surface quality can be maintained in all positions and reaches when applying the machining parameters validated by previous studies [3], [4]. In addition, the results are equal to those of JMs.

5.2 Series A

When comparing the IR-machined Vertical and Overhead specimens the dimensional deviations in length and width are smaller when machining vertical (ΔL = 0.34 mm, ΔW = 0.15 mm). The nominal-actual difference of height is smaller when machining overhead compared to Vertical (ΔH = 0.49 mm), Short Reach and Long Reach (ΔH = 0.09 mm). Reason for this can be the different robot axis configuration of the compared positions leading to smaller deviations when milling forces are introduced. Another reason can be found in the robot or workpiece support system which is loaded in two opposite directions while machining as lifting and pressing forces can cause different system reactions such as vibrations.

If the QDV is factored in, the previous explanation of smaller horizontal deviations but larger height differences is reinforced by the QDV of the Vertical specimens. At a closer look the larger height deviation when machining vertical is also represented in the QDV height criterium where the vertical value is double that of the overhead manufacturing. When the QDV optical and haptic surface roughness values are inspected, indicating higher values for the sidewalls of the Overhead specimen, the thesis of robot or support system reactions such as vibrations can be underlined. When comparing the QDV of JM with IR specimens, the JM with 21.94 shows 2.31 points (11%) higher results than the IR with 19.63.

The 3D scans show no significant difference between most areas, except for sidewall a. This goes hand in hand with the QDV optical and haptic surface roughness inspection of the short edge and the large length deviation of the overhead specimen which affects the short edge as well. Altogether the mentioned factors indicate lower machining quality for the Overhead compared to the Vertical machined specimen.

During the comparison of short and long reach specimens no significant difference of the dimensional deviations can be identified. On the one hand, the QDV of the short reach specimen is noticeably higher with variance

predominantly in the lateral criteria of the short and long edge.
When inspecting the 3D point clouds, this can statistically not be confirmed. On the other hand, the point cloud indicates a statistically significant difference between the short and long reach bottom areas which cannot be supported by neither the dimensional nor QDV analysis. To sum up the comparison between short and long reach, there is no difference in dimensions but in surface quality favouring the long reach position.
When the 3D point cloud assessment method is applied, the results can be evaluated from two different perspectives. From the timber machining point of view, the deviations are on a scale that is almost irrelevant for practice but conclusions like tool marks and wood defects can be drawn. From the geodetic perspective there is a need of development of a testing strategy similar to the Wilcoxon rank-sum test that fits the quality assessment of both domains.

5.3 Series B

When the reach is increased, the height deviation of both, x- and y-aligned specimens increased (mean increase = 1.03 mm) while length (mean increase = 0.28 mm) and width (mean increase = 0.32 mm) deviations are subject to measuring noise. This effect can be traced back to both, the robot accuracy as well as the inaccurate alignment of the worktable coordinate system that determines workpiece placement. The total QDV is also affected by the reach and increases almost linearly with rising reach (mean increase = 4.48 points). The increased height deviations with rising reach can be supported by the QDV height criterium for both alignments. When looking into detail of the laser profile scans and optical inspection of the specimens, fuzzy grain defect occur more often at short reach, while torn fibre defects are sighted more frequently at high reach. Apart from all that, the tool marks get clearer with increased reach.
The main difference between the milling of x- and y-aligned pockets is, that the turning point of the trajectories requires the robot to primarily change its reach (y-aligned) or to change its lateral position and rotate (x-aligned). In the case of x-aligned specimens, there is not only motion straight in the direction of the reach but also lateral, allowing mass inertia to gain relevance. This is clearly visible in the results, with the larger deviations in length for the x-aligned specimens compared to the y-aligned ones. The investigation of QDV values does support this argument with slightly higher lateral criterium short edge values for the x-aligned specimens. The width measurements on the other hand show similar deviations at minimum and maximum reach. The smaller lateral criterium long edge values indicate less geometrical irregularities of the long edge when they are x- aligned.
The measurement of the average surface roughness R_a indicates a surface with less deviations when machining y-aligned specimens due to the fact that the robot is primarily moving along one direction parallel to the y-axis.

6 CONCLUSION

This study proves that the larger workspace - one of the main benefits of IRs compared to JMs - can be fully utilised without loss in milling accuracy. The required machining quality measured by dimensional deviations is within the margins of both regulations and the JM produced reference specimens. The surface quality of the IR-machined specimens, in the vast majority of cases, remains higher than the JM-produced reference specimens. To sum up, the following observations need to be particularly highlighted:

- The required machining accuracy and surface quality can be maintained in all investigated positions of Series A and B and levels of reach while the results are of higher or equal quality compared to those of a JM.
- The comparison of vertical and overhead machining of Series A reveals slightly higher quality results in terms of horizontal dimensions and surface quality for vertical machining.
- When comparing the opposite short and long reach specimens of Series A, no clear dimensional difference was found, yet the surface quality was higher when machining long reach specimens.
- The dimensional deviations, surface deviations and irregularities (QDV) of specimens machined with identical tool orientation increases when the robots´ reach is increased.
- The dimensional and surface (QDV) quality is decreased when the robot machining trajectories are primarily lateral (x-aligned) compared to primarily longitudinal (y-aligned).

Further research is planned on the machining accuracy of different robot positions in the workspace. For this the location of the tool centre point tracked by ABB´s online signal analysis will be compared with the accuracy of machining results measured by the laser profile scanner.

ACKNOWLEDGEMENT

The authors would like to show their gratitude to Rubner Holzbau GmbH, Leitz GmbH & Co. KG and the Research Unit of Engineering Geodesy at TU Wien for the cooperation. The project is grant by the Austrian Research Promotion Agency (FFG) (project no. 878081).

REFERENCES

[1] International Federation of Robotics, “World Robotics 2021,” Oct. 28, 2021.
[2] M. Pantscharowitsch and B. Kromoser, “Automated Subtractive Timber Manufacturing – Joinery Machines vs. Industrial Robots,” *Journal of Manufacturing Science and Engineering*, 2022.
[3] M. Pantscharowitsch and B. Kromoser, “Influence of Machining Parameters on Subtractive Manufacturing of Elementary Geometries in Glued Laminated Timber Using an Industrial Robot,” *Wood Material Science and Engineering*, p. 37, 2021.
[4] M. Pantscharowitsch and B. Kromoser, “Investigation of Industrial Robots vs. Joinery Machines for Milling Pockets in Glulam –

https://doi.org/10.52202/069179-0082

Comparison Based on Surface Quality and 3D Scans," *Civil Engineering Design - Conference (Green Civil Engineering 2022)*, 2022.
[5] M. Pantscharowitsch and B. Kromoser, "Milling Tenons on GLT Beams Using an Industrial Robot and Joinery Machine – Comparison Based on Surface Quality and 3D Scans," Portland, OR, 14-04 2022.
[6] B. Kromoser, M. Braun, and M. Ortner, "Construction of All-Wood Trusses with Plywood Nodes and Wooden Pegs: A Strategy towards Resource-Efficient Timber Construction," *Applied Sciences*, vol. 11, no. 6, p. 2568, Mar. 2021, doi: 10.3390/app11062568.
[7] W. Piatke, "Interview: Wolfgang Piatke, Vertriebsleiter Hundegger AG," Jan. 14, 2021.
[8] CEN, Austrian Standards, *EN 336:2013 10 - IDT - Structural timber - Sizes, permitted deviations*.
[9] CEN, Austrian Standards, *Önorm EN 1995-1-1:2010-12 Eurocode 5: Design of timber structures - Part 1-1: General - Common rules and rules for buildings*. Brussels: European Committee for Standardization, 2010.
[10] CEN, *ÖNORM EN 14080: 2013 08 01: Timber structures - Glued laminated timber and glued solid timber - Requirements*. Brussels: European Committee for Standardization, 2013.
[11] L. Gurau and M. Irle, "Surface Roughness Evaluation Methods for Wood Products: a Review," *Curr Forestry Rep*, vol. 3, no. 2, pp. 119–131, Jun. 2017, doi: 10.1007/s40725-017-0053-4.
[12] Forest Products Laboratory, "Raised, Loosened, Torn, Chipped and Fuzzy Grain in Lumber." US Forest Service, 1955.
[13] CEN, *ÖNORM EN ISO 4287:2012 02 01 - Geometrical Product Specifiations (GPS) - Surface Texture: Profile Method- Terms, Definitions and Surface Texture Parameters*, vol. 4287:2012 02. 2012.
[14] CEN, *ÖNORM EN ISO 16610-21:2013 07 01 - Geometrical product specifications (GPS) - Filtration Part 21*. 2013.